THE ASTROPHYSICAL JOURNAL, 420:L5–L8, 1994 January 1

INFRARED OBSERVATIONS OF THE $z = 3.8$ RADIO GALAXY, 4C 41.17, WITH THE W. M. KECK TELESCOPE

JAMES R. GRAHAM,[1,2] K. MATTHEWS,[3] B. T. SOIFER,[3] J. E. NELSON,[1,4] W. HARRISON,[4] J. G. JERNIGAN,[5] S. LIN,[3] G. NEUGEBAUER,[3] G. SMITH,[4] AND C. ZIOMKOWSKI[3]

Received 1993 July 14; accepted 1993 October 12

ABSTRACT

The near-infrared camera on the W. M. Keck telescope has been used to image the $z = 3.8$ radio galaxy 4C 41.17. The 2 μm continuum consists of a thin arc of emission aligned along the radio axis. There is close correlation between the optical, infrared, and radio emission. The color of 4C 41.17 is blue ($R-K_S = 2.7 \pm 0.1$ mag). This may indicate ongoing star formation, but the origin of the continuum emission remains unclear. [O III] and Hβ emission makes a large contribution to the K-band flux. A number of faint red companions of 4C 41.17 are detected in the 2 μm image. If these sources are at the same redshift as 4C 41.17, then their red colors indicate ages of more than $\sim$0.5 Gyr and an epoch of formation at $z \gtrsim 8$.

Subject headings: early universe — galaxies: active — galaxies: formation — radio continuum: galaxies

1. INTRODUCTION

Several galaxies with redshifts in the range 3–4 are now known. These galaxies are young, because for a wide range of cosmological parameters they have ages of less than $\sim$20% of the current age of the universe. Large telescopes allow detailed studies of distant galaxies, and therefore offer a window on the epoch of galaxy formation. Here we present some of the first observations made with the 10 m W. M. Keck telescope on Mauna Kea, Hawaii: infrared imaging of the most distant known galaxy 4C 41.17, at $z = 3.8$ (Chambers, Miley, & van Breugel 1990).

4C 41.17 is a steep spectrum radio galaxy, with a F-R II morphology. The central radio source is coincident with a large ($\gtrsim$70 kpc) Lyα cloud. The Lyα and UV continuum are fairly well aligned with the radio emission. The galaxy is relatively bright at 2.2 μm, although little is known about the morphology (Chambers et al. 1990). High-resolution *Hubble Space Telescope* images of 4C 41.17 show that the R-band emission is clumpy with a morphology that correlates with the radio on sub-kiloparsec scales (Miley et al. 1992).

2. OBSERVATIONS AND REDUCTIONS

4C 41.17 was observed on 1993 March 24 and 25 using the 10 m W. M. Keck telescope with the facility near-infrared camera (Matthews et al. 1994). The camera is equipped with a SBRC 256 × 256 InSb array. The pixel size is 0.″15. We observed at K (2.0–2.4 μm) and K_S (2.0–2.3 μm), the former includes redshifted [O III] and Hβ. An integration time of 21 s yields background-limited performance, while preventing saturation. Frames were obtained in groups of five and then the telescope was repositioned by a few arcseconds. Each frame was guided using an off-axis CCD camera. The exposure time for the central 40″ of the resultant mosaic is 2372 s and 1386 s at K_S and K, respectively.

All frames were sky subtracted and then flat fielded using dark subtracted sky frames. The positions of two to three stars in each frame were used for spatial registration. Photometry was performed relative to UKIRT faint standards (Casali & Hawarden 1992). The K_S magnitudes of these stars are unknown. However, we chose blue standards, and adopted $K-K_S = 0$ mag. The resultant photometric error should be less than 2%. Figure 1 (Plate L2) is a finding chart for each object in the field, and Figure 2 is the color-magnitude diagram derived from the photometry listed in Table 1.

A 1200 s exposure R-band CCD image of 4C 41.17, obtained at the 4 m telescope of the Kitt Peak National Observatory in 1989 March, was provided by Dickinson & Spinrad (1993).

The positions of five stars present in the infrared and the R-band images were used to transform all the observations to a common coordinate frame. Astrometry of stars common to the Palomar Sky Survey and the R-band image permits us to establish absolute coordinates. The relative registration of the optical and infrared images is good to 0.″1, and the absolute coordinates are accurate to 0.″5.

3. RESULTS

The K_S mosaic achieves a 1 σ limiting magnitude of 23.1 mag in a 3″ diameter beam. The image size is seeing limited with a full width at half-maximum (FWHM) of 0.″87. The K mosaic limit is 22.7 mag, 1 σ, in the same-sized beam, and the FWHM is 0.″65. The R images have 26.9 mag. 1 σ and FWHM = 0.″9.

The K_S image (Figs. 3 [Plate L3] and 4) shows that 4C 41.17 consists of a single nucleus at the center of a thin curved arc of emission that extends over $\simeq$6″ or 26 kpc ($H_0 = 75$ km s^{-1} Mpc^{-1}, $q_0 = 0.5$). The arc is clumpy, a conclusion that is reinforced by a K_S mosaic with FWHM of 0.″6 constructed by selecting 50 images with the best seeing. There is a marked concentration of faint ($K_S \simeq$ 20–23 mag) objects near 4C 41.17 of which only the brightest has been previously detected (object 12 is object Z of Chambers et al. 1990). At least seven such objects (2–5, 9, and 12) are located within a radius of 12″ (53 kpc). All the objects are resolved.

Infrared spectra of 4C 41.17 show that the K_S filter band pass is free of bright emission lines (Eales & Rawlings 1993),

[1] Astronomy Department, University of California, Berkeley, CA 94720.
[2] Alfred P. Sloan Research Fellow.
[3] Palomar Observatory, California Institute of Technology, Pasadena, CA 91125.
[4] California Association for Research in Astronomy, 65-1120 Mamalahoa Highway, P.O. Box 220, Kamuela, HI 96743.
[5] Space Sciences Lab, University of California, Berkeley, CA 94720.

PLATE L2

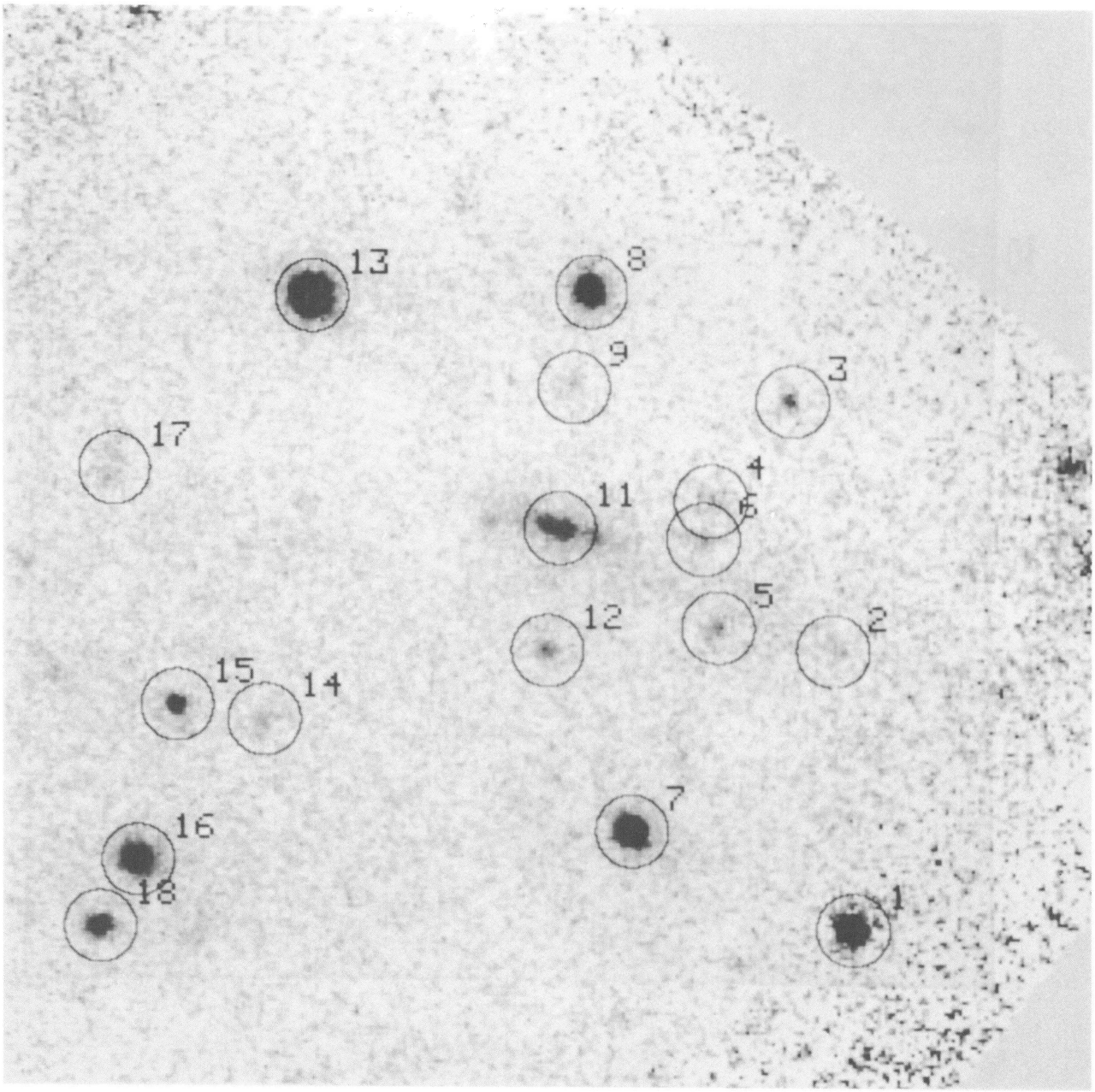

FIG. 1.—Finding chart for the objects shown in Fig. 2 overlaid on the *K* image of 4C 41.17 (object 11). The field of view is ~45″ on a side. North is at the top, and east to the left. The circles have a diameter of 3″.

GRAHAM et al. (see 420, L5)

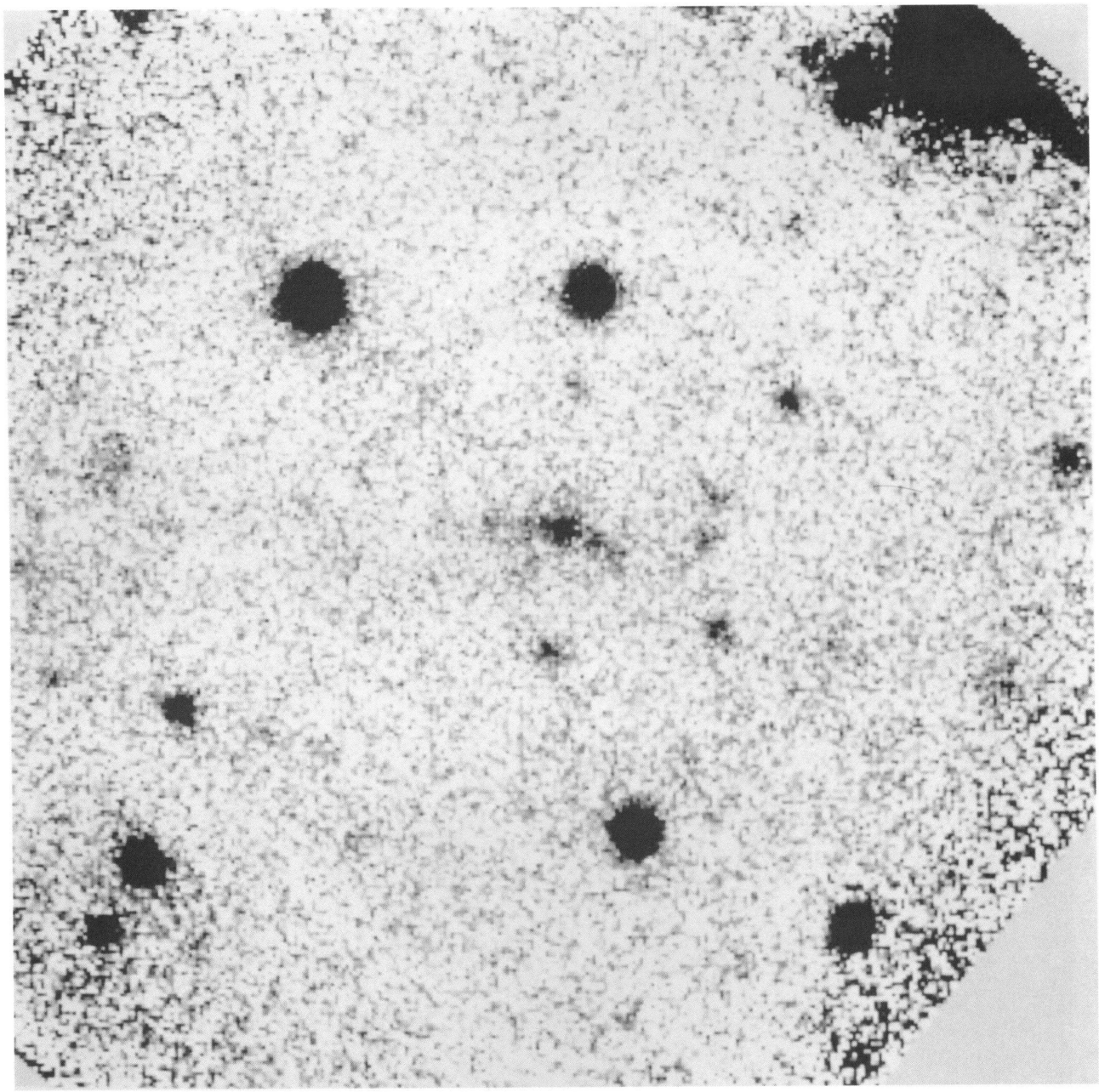

FIG. 3.—Linear gray-scale representation of the K_S image of 4C 41.17. The field of view is $\sim 45''$ on a side. North is at the top, and east to the left.

GRAHAM et al. (see 420, L5)

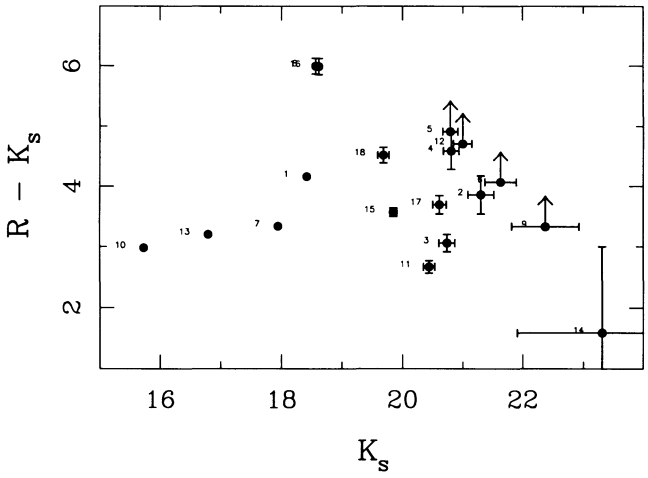

FIG. 2.—Color magnitude diagram for the field of 4C 41.17. The number beside the symbol refers to the identification in Fig. 1.

therefore K_S gives a good measure of the continuum. In a 4″ diameter beam, 4C 41.17 has $K_S = 19.6 \pm 0.6$ mag, substantially brighter than the radio galaxy B2 0902+34 ($K \simeq 21.5$ mag, $z = 3.4$) (Eisenhardt & Dickinson 1992). At $z = 3.8$ the observed K band corresponds to the rest frame B, and the K_S magnitude can be converted directly into $M_B = -23.0$ mag. An L^* galaxy at $z = 3.8$ has $K = 23.1$ mag (if $M_B^* = -19.7$ mag), so all the faint objects in the vicinity of 4C 41.17 are more luminous than L^* if they are at the same distance.

TABLE 1

PHOTOMETRY[a]

Object	K	Error	K_S	Error	$R-K_S$	Error
1.....	18.08	0.04	18.43	0.03	4.16	0.04
2.....	21.14	0.31	21.30	0.22	3.86	0.32
3.....	20.65	0.26	20.73	0.13	3.06	0.14
4.....	20.80	0.22	20.80	0.13	4.59	0.30
5.....	21.45	0.37	20.79	0.12	4.91	...
6.....	21.17	0.28	21.63	0.26	4.07	...
7.....	17.80	0.01	17.95	0.01	3.33	0.01
8.....	18.41	0.03	18.57	0.02	6.00	0.13
9.....	22.29	0.78	22.37	0.55	3.33	...
10.....	15.54	0.00	15.73	0.00	2.98	0.00
11[b].....	19.06	0.04	20.44	0.09	2.67	0.10
12.....	20.83	0.17	20.99	0.15	4.71	...
13.....	16.67	0.00	16.80	0.00	3.20	0.01
14.....	21.63	0.37	23.31	1.40	1.59	1.41
15.....	19.78	0.07	19.85	0.06	3.57	0.07
16.....	18.41	0.02	18.62	0.03	5.99	0.13
17.....	21.05	0.22	20.61	0.11	3.69	0.15
18.....	19.46	0.06	19.68	0.09	4.52	0.13

[a] In a 3″ circular aperture. Errors include only the statistical uncertainty. The absence of an entry in the error column indicates a 3 σ upper limit.
[b] Nucleus of 4C 41.17.

At K (Figs. 4 and 5 [Plate L4]) the nuclear region of 4C 41.17 appears as a double source separated by 0.″65. The two K peaks straddle the K_S nucleus. The difference between the K and K_S morphology is due to redshifted Hβ and [O III] present in the K filter band pass. The distribution of K light, like K_S, is clumpy, and the two bright knots in the main body of the

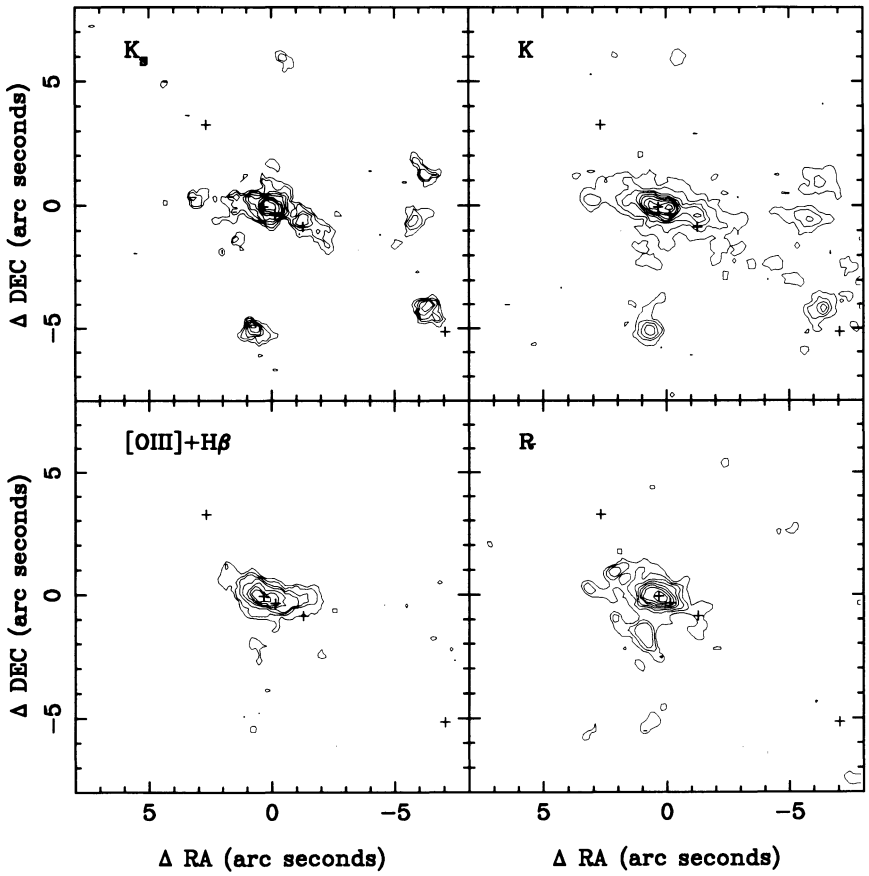

FIG. 4.—Contour plots of K_S, K, and [O III] + Hβ and R images of 4C 41.17. The positions of the main radio components, A, B_1, B_3, and C (from west to east), as identified by Chambers et al. (1990), are shown as crosses.

PLATE L4

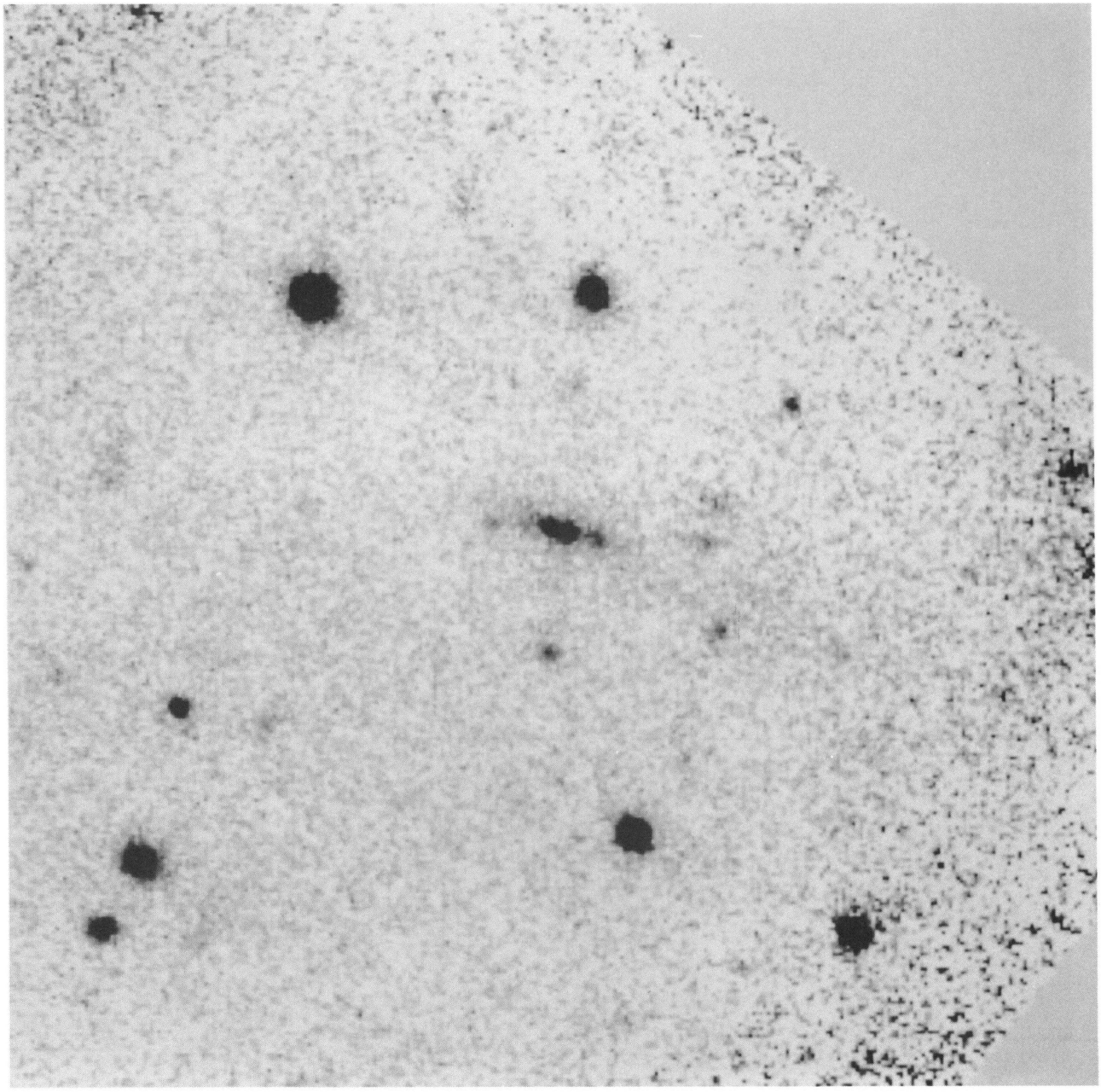

FIG. 5.—Linear gray-scale representation of the *K* image of 4C 41.17. The field of view is ~45″ on a side. North is at the top, and east to the left.

GRAHAM et al. (see 420, L6)

galaxy, seen in the K_S image, are also present at K. All the faint companions also appear in the K image, and low surface brightness emission runs from the main body of the galaxy along the radio axis toward radio component A, and to the south. Figure 6 [Plate L5] shows the R-band image.

A Hβ+[O III] line emission image can be constructed by subtracting the K_S image from K. The resultant image (Fig. 4) has a band pass of 2.3–2.4 μm. Before subtraction the K and K_S images were smoothed to the same spatial resolution. The resultant image shows a comma-shaped emission-line knot. Although the nebula is generally aligned along the radio axis, it shows a distinct curvature away from the radio axis toward an east-west direction, reminiscent of the Lyα halo. Unlike the original K image the Hβ+[O III] image shows a single peak. Because the K image was smoothed before subtraction, the resolution of the Hβ+[O III] image is too low to resolve these peaks, but the line emission image still suggests a double structure. The best-seeing Lyα image of Chambers et al. (1990) has a resolution of 1".0 FWHM and shows only a single peak. None of the weaker knots in the body of the galaxy, or any of the nearby companion sources are detected in the line emission image. The faint emission which runs along the radio axis at K is just visible in the Hβ+[O III] image. This emission is harder to discern because of the additional $\simeq 2^{1/2}$ noise in the difference image.

3.1. *Comparison with Radio and Optical*

None of the infrared sources is precisely coincident with a radio source—and it might be fortuitous if one was, due to the uncertainty between optical and radio reference frames—but there is a clear association and alignment between radio and infrared emission. High-redshift ($0.6 < z < 2$) radio galaxies exhibit elongated optical emission which is closely aligned with the axes defined by their radio lobes (McCarthy et al. 1987; Chambers et al. 1987). Since the K_S band samples the rest frame B, the preferential orientation of the 2 μm light along the radio axis shows that, even at the highest redshifts, the alignment effect is present in the rest frame visible light. This suggests that common mechanisms determine the morphology of radio galaxies between $z \simeq 0.6$ and $z \simeq 4$. Comparison of the K, K_S, and R images suggests that the alignment of emission along the radio axis is most pronounced at 2 μm. Compared to the elongated K_S image, the R-band emission is amorphous.

The positions of the main radio components, A, B_1, B_2, B_3, and C, as identified by Chambers et al. (1990), are shown as crosses on contour plots (Fig. 4). The K_S peak lies close (0".3 west) to radio peak B_3. The two K peaks straddle B_3, and the western K peak is only slightly offset from the weak radio core B_2. Source B_1 lies in the arc of emission that defines the body of the galaxy, and is next to a clump present in the K_S and K images. One newly detected infrared companion (source 5) is close to radio component A (0".8 east, 1".0 north) and falls along the axis defined by the radio sources. No infrared counterpart of radio source C is detected.

Comparison of the K and K_S images with the *Hubble Space Telescope* image of 4C 41.17 by Miley et al. (1992) in the F702W filter reveals close similarities. The K_S peak is coincident with the *HST* component H_4. The K_S nuclear contours are extended along the position angle joining H_2 and H_4, suggesting that a second peak, at the location of H_2, might be resolved at K_S in better seeing. The western K nucleus is accurately aligned with feature H_2. The eastern nucleus does not correspond to a *HST* peak, but to resolved emission that extends to the east. The two weaker K_S and K sources in the main body of the galaxy also align with structure seen in the *HST* image: the 2 μm peak 1" west of the K_S nucleus lines up with H_1, while the 2 μm source 3" east of the nucleus appears in the *HST* image (this source is outside of the field of view displayed by Miley et al. 1993).

If we shift the radio reference frame 0".3 north relative to the optical one, so that B_2 and B_3 coincide with H_2 and H_4 (cf. Miley et al. 1992) then the correlation between the radio and infrared improves. The western K nucleus now lines up accurately with B_2, and the alignment with B_1 is closer.

Observations of 4C 41.17 reveal a remarkable small-scale ($\sim$500 pc) correlation between emission seen in the rest frame UV, blue, and radio. This correlation suggests that it is unlikely that the emission is scattered light from beamed nuclear emission. The clear curvature of the K_S image reinforces this conclusion. There is good correlation between the radio, optical, and infrared, but the correlation is not complete. There is no radio source associated with the knot of emission 3" east of the nucleus, and no optical or infrared emission associated with radio source C. This may provide some difficulties for the inverse Compton model (Daly 1992).

3.2. *Contribution of Line Emission*

The large difference between K and K_S, $K_S - K = 0.9 \pm 0.06$ mag shows that the 2 μm light is severely contaminated by bright emission lines. This implies that $64 \pm 6\%$ of the K light measured in a 4" diameter beam is due to Hβ and [O III]. A significant fraction of the K-band light is due to line emission—much larger than the 15% measured by Eales & Rawlings (1993). The Eales & Rawlings measurement relies on comparing slit spectroscopy with published photometry. If we compare Eales & Rawlings's [O III] flux in a 3" diameter beam with the K flux, then the fraction of [O III] is $40\% \pm 10\%$. Hβ probably contributes another $\simeq$10%, and therefore most of the discrepancy is resolved.

4C 41.17 is similar to other high-redshift radio galaxies where the K-band magnitudes are significantly perturbed by line emission (Eisenhardt & Dickinson 1992; Eales & Rawlings 1993). The infrared magnitudes of high-redshift galaxies are vital for deciding the cosmological status of these young objects. Red optical-infrared colors would suggest the presence of large numbers of giants and imply an evolved population indicative of an early epoch of formation (Lilly 1988, 1989; Chambers & Charlot 1990). If line emission dominates broad-band magnitudes then this factor must be taken into account when interpreting the K Hubble diagram (cf. Eales & Rawlings 1993).

3.3. *Colors and Number Counts*

Figure 2 shows a color-magnitude diagram for the field of 4C 41.17. 4C 41.17 is the bluest non-stellar object in the field. The nature of the UV-optical continuum emission in radio galaxies is uncertain. The high degree of polarization suggests that scattered nuclear light may contribute to the observed continuum in some objects (Di Serego Alighieri et al. 1989; Jannuzi & Elston 1991; Tadhunter et al. 1992). Spinrad et al. (1993) report a strong Lyman continuum break in 4C 41.17, which is good evidence for a stellar origin for the UV light. If the R and K_S band light is starlight, is the blue color evidence that 4C 41.17 is a primeval galaxy forming its first generation of stars? For 4C 41.17, $R - K_S = 2.7 \pm 0.1$ mag in a 3" diameter beam. Eisenhardt & Dickinson (1992) argued that B2

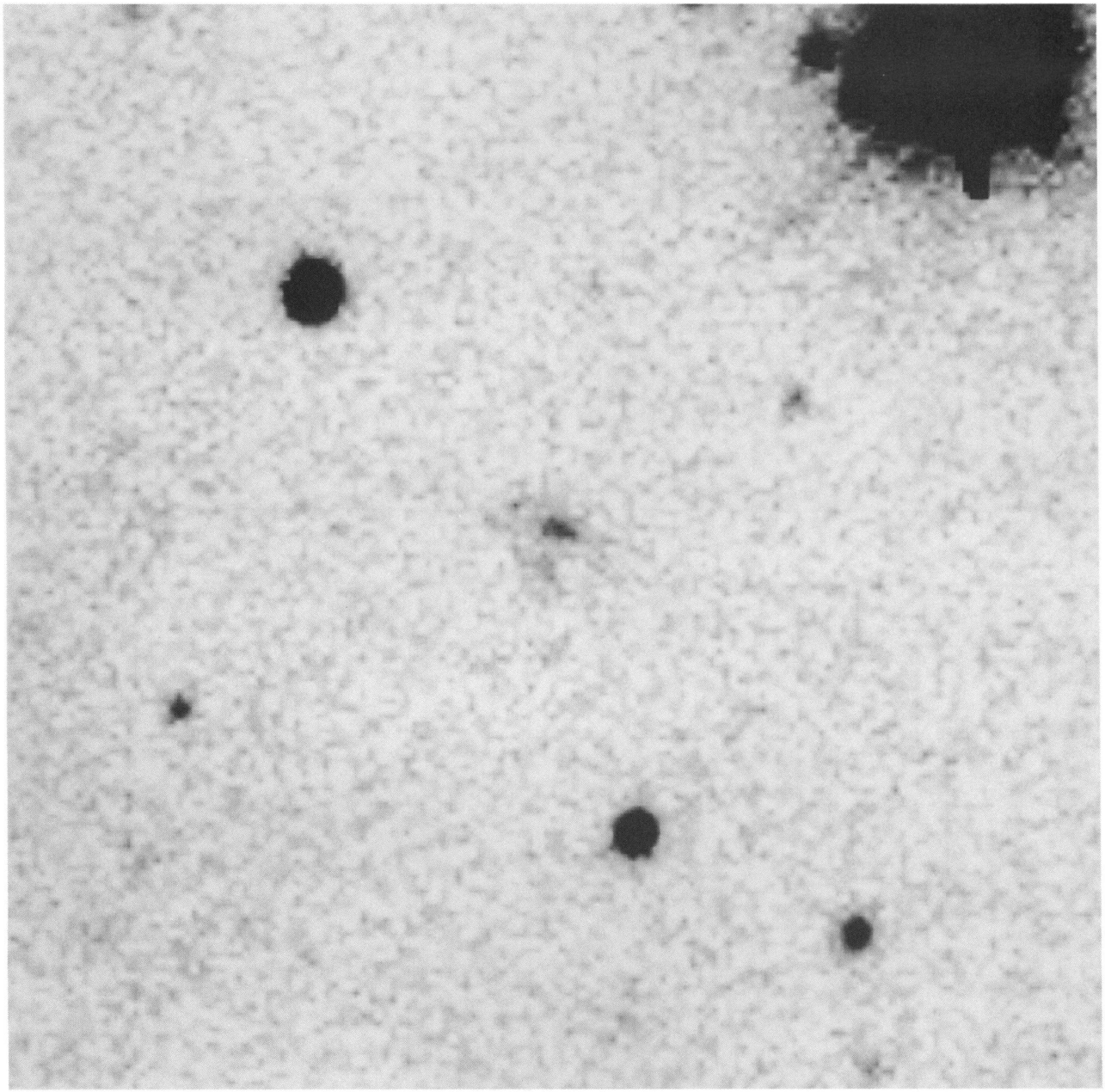

FIG. 6.—Linear gray scale representation of the *R* image of 4C 41.17. The field of view is ~45″ on a side. North is at the top, and east to the left.

GRAHAM et al. (see 420, L7)

0902+34, with $R-K = 1.9^{+1.1}_{-\infty}$, has a spectrum characteristic of a protogalaxy. For comparison we have calculated the colors of galaxies redshifted to $z = 3.8$, using the model spectral energy distributions of Bruzual & Charlot (1993). These yield $R-K_S = 7.33$, 3.95, 3.07, and 2.21 mag for E, Sb, Sc, and Im galaxies, respectively. The $R-K_S$ color of 4C 41.17 falls between the Sc and Im. The $R-K_S$ color of 4C 41.17 is therefore characteristic of a stellar population which has recent or ongoing star formation. Since the R-band corresponds to rest frame ultraviolet, the reddening correction to the observed $R-K_S$ color is large, $1.8A_V$ (Matthis 1990). Consequently even a small amount of dust can significantly effect the observed color.

To place limits on the age of 4C 41.17 we have calculated the colors of stellar populations formed in an instantaneous burst and by continuous star formation using the galaxy isochrone synthesis library of Bruzual & Charlot (1993). The models assume a Salpeter initial mass function between 0.1 and 125 $M_\odot$ and solar metallicity and no reddening. Comparison of the calculated colors as a function of time with the observed colors places two extreme limits on the age. The instantaneous starburst matches the observed color after 0.07 Gyr, while continuous star formation must proceed for 10 Gyr to achieve the observed color. In consequence, the limits on the age of 4C 41.17 are very poor, and it is premature to draw conclusions about the age of the stellar population of 4C 41.17.

Object 3 is the next bluest object, after 4C 41.17, with $R-K_S = 3.1$ mag, and only 14, 15, and 17 have $R-K_S < 4$ mag. The closest companions of 4C 41.17 (4–6, 9, and 12) are distinctly red. For example, object 5, the source adjacent to radio component A, and therefore most likely at the same redshift as 4C 41.17, has $R-K_S > 5$ mag. The emission from these sources is most likely starlight, since, with the exception of object 5, they are not coincident with radio sources, or aligned along the radio jet. Comparison with the colors of an instantaneous star burst indicates a lower limit on the age of about 0.5 Gyr. If the faint companions of 4C 41.17 are at $z = 3.8$ then their inferred age implies formation at $z \gtrsim 8$.

The color magnitude diagram for the field of 4C 41.17 (Fig. 2) contains two very red galaxies (objects 8 and 16). Both have $K = 18.41 \pm 0.03$ mag and $R-K = 6.16 \pm 0.13$ mag and 6.20 ± 0.13 mag, respectively. Both objects are galaxies since they are resolved with a FWHM $\simeq 0\farcs5$. The colors are those of an unevolved elliptical galaxy at $z \simeq 1.1$. Normal spirals galaxies never exhibit such red colors. The presence of two such galaxies suggests that this is not a coincidence, and that we may be viewing 4C 41.17 through a foreground cluster. If $M^*_B = -19.7$ mag, then at $z \simeq 1.1$, these galaxies correspond to $\simeq 1.6L^*$, and therefore would rank among the brighter cluster members. Inspection of the number vs. magnitude counts shows an excess of galaxies in the magnitude range 18–19 compared with the counts of Cowie et al. (1993). This observation is consistent with the suggestion that catalogs of the most distant radio galaxies are affected by selection effects due to gravitational lensing and amplification (Hammer & Le Fèvre 1990).

The W. M. Keck Observatory is a scientific partnership between the University of California and the California Institute of Technology, made possible by the generous gift of the W. M. Keck Foundation and support of its president, Howard Keck. We are most grateful for their visionary endowment that has made possible the first of the next generation of telescopes. It is a pleasure to thank E. Stone, W. Frazier, W. Sargent, S. Faber, E. Romano, and W. Lupton and all of the many devoted people whose unflagging efforts have made possible the success of the W. M. Keck Observatory.

We thank M. Dickinson and H. Spinrad for permission to use their R-band image of 4C 41.17. Thanks are also due to M. Dickinson for advice and practical help on data reduction and valuable discussions on the nature of high-redshift radio galaxies.

REFERENCES

Bruzual, G., & Charlot, S. 1993, ApJ, 405, 538
Casali, M. M., & Hawarden, T. G. 1992, JCMT-UKIRT Newsletter, 4, 33
Chambers, K. C., Miley, G. K., & van Breugel, W. J. M. 1987, Nature, 329, 604
———. 1990, ApJ, 363, 21
Cowie, L. L., Gardner, J. P., Hu, E. M., Wainscoat, R. J., & Hodapp, K. W. 1993, ApJ, submitted
Daly, R. A. 1992, ApJ, 399, 426
Dickinson, M., & Spinrad, H. 1993, private communication
Di Serego Alighieri, S., Fosbury, R. A. E., Quinn, P. J., & Tadhunter, C. N. 1989, Nature, 341, 307
Eales, S. A., & Rawlings, S. 1993, ApJ, 411, 67
Eisenhardt, P., & Dickinson, M. 1992, ApJ, 399, L47
Hammer, F., & Le Fèvre, O. 1990, ApJ, 357, 38
Jannuzi, B. T., & Elston, R. 1991, ApJ, 366, L69
Lilly, S. J. 1988, ApJ, 333, 161
———. 1989, ApJ, 340, 77
Mathis, J. S. 1990, ARA&A, 28, 37
Matthews, K., et al. 1994, in Proc. UCLA Conf. on Infrared Detector Arrays, ed. I. McLean & G. Brims (Dordrecht: Kluwer), in press
McCarthy, P. J., van Breugel, W. J. M., Spinrad, H., & Djorgovski, S. G. 1987, ApJ, 321, L29
Miley, G. K., Chambers, K. C., van Breugel, W. J. M., & Macchetto, F. 1992, ApJ, 401, L69
Spinrad, H., Dickinson, M., Schlegel, D., & Gonzalez, R. 1993, in Observational Cosmology, ed. G. Chincarini, T. Maccacaro, & D. Maccagni, in press
Tadhunter, C. N., Scarrott, S. M., Draper, P., & Rolph, C. 1992, MNRAS, 256, 53p